
Article:
Nedelkoski, Z., Kepaptsoglou, D. orcid.org/0000-0003-0499-0470, Ghasemi, A. et al. (7 more authors) (2016) Controlling the half-metallicity of Heusler/Si(1 1 1) interfaces by a monolayer of Si-Co-Si. Journal of physics : Condensed matter. 395003. pp. 1-6. ISSN 1361-648X

https://doi.org/10.1088/0953-8984/28/39/395003

Controlling the half-metallicity of Heusler/Si(1 1 1) interfaces by a monolayer of Si–Co–Si

2016 J. Phys.: Condens. Matter 28 395003

OPEN ACCESS
IOP Publishing
Journal of Physics: Condensed Matter
J. Phys.: Condens. Matter **28** (2016) 395003 (6pp)
doi:10.1088/0953-8984/28/39/395003

Controlling the half-metallicity of Heusler/Si(1 1 1) interfaces by a monolayer of Si–Co–Si

Zlatko Nedelkoski[1], Demie Kepaptsoglou[2], Arsham Ghasemi[1], Balati Kuerbanjiang[1], Philip J Hasnip[1], Shinya Yamada[3], Kohei Hamaya[3], Quentin M Ramasse[2], Atsufumi Hirohata[4] and Vlado K Lazarov[1]

[1] Department of Physics, University of York, Heslington, York, YO10 5DD, UK
[2] SuperSTEM Laboratory, SciTech Daresbury Campus, Daresbury WA4 4AD, UK
[3] Department of Systems Innovation, Osaka University, Osaka 560-8531, Japan
[4] Department of Electronics, University of York, York, YO10 5DD, UK

E-mail: vlado.lazarov@york.ac.uk

Received 7 July 2016, revised 20 July 2016
Accepted for publication 22 July 2016
Published 9 August 2016

Abstract

By using first-principles calculations we show that the spin-polarization reverses its sign at atomically abrupt interfaces between the half-metallic Co_2(Fe,Mn)(Al,Si) and Si(1 1 1). This unfavourable spin-electronic configuration at the Fermi-level can be completely removed by introducing a Si–Co–Si monolayer at the interface. In addition, this interfacial monolayer shifts the Fermi-level from the valence band edge close to the conduction band edge of Si. We show that such a layer is energetically favourable to exist at the interface. This was further confirmed by direct observations of $CoSi_2$ nano-islands at the interface, by employing atomic resolution scanning transmission electron microscopy.

Keywords: half-metals, spintronics, Heusler alloys, spin-injection

S Online supplementary data available from stacks.iop.org/JPhysCM/28/395003/mmedia

(Some figures may appear in colour only in the online journal)

Introduction

Efficient spin injection from ferromagnets into Si, as a mainstream semiconductor, is a key requirement for the development of low power and high speed spin-based electronics [1–4]. One of the biggest challenges for achieving efficient spin injection into semiconductors in general is the conductivity mismatch between ferromagnets and semiconductors [5]. One way to overcome this obstacle is to use 100% spin-polarized electrodes i.e. half-metallic materials [5]. Several Co-based Heusler alloys such as Co_2FeSi (CFS), Co_2MnSi (CMS), Co_2Fe(Si,Al) (CFAS), all predicted by density functional theory (DFT) calculations as 100% spin-polarized materials, have been already implemented in a number of heterostructured spintronic devices [6–14]. We would like to note that the correlation between the calculated spin-polarization (SP) by DFT and the measured SP indirectly through transport device parameters or optical methods is not straightforward and requires careful consideration of several phenomena that arise from temperature effects, such as magnon and phonon effects etc [15]. In addition to the predicted 100% SP at the Fermi-level, these full-Heusler alloys have a very high magnetic moment (4–6 μ_B/per formula unit) and Curie temperature (900–1100 K) [3]. These properties make the Co-based Heusler alloys ideal candidates for implementation in various spintronic devices including hybrid devices based on Si. In order to exploit their half-metallicity, it is crucial to preserve their atomic and electronic structure not only in the bulk-like part of the electrode but also at the interface with the semiconductor (e.g. Si) with the ultimate goal to retain the 100% SP.

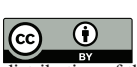

The control of the atomic structure at the Heusler/Si interfaces has been very challenging and the major obstacle that has hampered the progress of very efficient spin injection into Si. Recent progress in growth has shown that the quality of these interfaces can be greatly improved, i.e. the spatial extent of the diffusion can be limited to a very narrow interface region [16]. However, even for ideal half-metallic electrodes and atomically abrupt interfaces, DFT studies predict a reduction of the SP in the vicinity of the interface, as reported for Heusler/GaAs and Heusler/Ag interfaces in [17–19]. In other words, structural and chemical abruptness of the interface does not necessarily lead to an interface electronic structure desirable for spintronic devices. Therefore, it is of fundamental interest to study the interface atomic structure's influence on the SP and consequently determine interface atomic configurations which retain a high SP.

In this letter, we employ first-principles calculations to show that the atomically sharp CFS(1 1 1)/Si(1 1 1) interface has reversed SP at the interface. This dramatic sign change of the SP at the Fermi-level from positive to negative at the interface could be detrimental for the spin injection efficiency. This unfavourable spin-electronic configuration can be avoided completely by introducing a Si–Co–Si monolayer at the interface. The unexpected phenomenon of SP reversal has been also confirmed for CFAS and CMS films. Moreover, we show that in all studied interfaces, i.e. Co_2(Fe,Mn)(Al,Si)/Si–Co–Si/Si(1 1 1), the Si–Co–Si monolayer maintains the positive SP right up to the interface. It is worth noting that the $CoSi_2$ phase is the end product when Si substitutes all Fe atoms in CFS, a process likely to be achieved due to the diffusion of Si into the Heusler electrode. Indeed, we find $CoSi_2$ experimentally in the form of interfacial nanoislands, several atoms thick, fully epitaxially interwoven between the Si and CFAS Heusler electrode. These results confirm that the interfacial structure determined as Co_2(Fe,Mn)(Al,Si)/Si–Co–Si/Si(1 1 1) is thermodynamically stable, hence can be a target for subsequent studies of engineering interface structure with high spin polarisation.

Methods

Density functional theory (DFT) calculations were performed using the CASTEP [20] code on periodically repeating supercells constructed from six Si and eight CFS unit cells along the [1 1 1] direction. The lateral (in the interface plane) lattice parameters were fixed while the perpendicular lattice parameter and the atomic coordinates were geometrically optimized. A PBE + U exchange-correlation functional was used, with a Hubbard U term of 2.1 eV for both d-block elements Co and Fe [21]. This value for U has previously been shown to open up the minority band-gap, approximately correcting for the delocalising effect of self-interaction with PBE alone [22]. Ultrasoft PBE pseudopotentials were used with a plane wave cut-off energy of 600 eV. The Brillouin zone was sampled using a Monkhorst–Pack grid with a *k*-point sampling spacing of 0.03 2π Å^{-1}. Partial density of states (PDOS) were calculated using the OPTADOS [23] code with the fixed Gaussian broadening scheme. The potential—sum of the local part of the pseudo potential, Hartree term and exchange term, averaged in-plane and along z over the unit cells of Si and CFS, is plotted along the direction normal to the interface plane. Valence band edges are calculated separately for bulk Si and CFS with respect to their averaged potential, and then offset for the calculated potential difference across the interface [24].

The CFAS thin film was prepared by co-deposition of Co, Fe, Si and Al using low-temperature molecular beam epitaxy [25]. A 25 nm thick CFAS film was deposited on a pre-cleaned $10 \times 10\,\text{mm}^2$ Si(1 1 1) substrate at room temperature. Cross-sectional transmission electron microscopy samples were prepared by conventional methods that include mechanical thinning and finishing with Ar-ion milling [26], as well as by focused-ion-beam (FIB). Atomic-level structural studies were performed by aberration-corrected (AC) scanning transmission electron microscopy (STEM) using high-angle-annular-dark-field (HAADF) imaging on a Nion UltraSTEM 100 microscope [27].

Results and discussion

We start with presenting the results for an atomically abrupt CFS/Si interface. Both the CFS film and the Si substrate are oriented along the [1 1 1] crystallographic direction. In addition to the shared [1 1 1] direction, the following epitaxial crystallographic relationships are satisfied: CFS(1−10)||Si(−1 1 0) and CFS(11−2)||Si(11−2). This epitaxy in turn allows construction of a supercell model with lateral dimensions equal to the Si(1 1 1), or equally to the CFS(1 1 1) in-plane lattice parameters. Along the [1 1 1] crystallographic direction, the bulk CFS structure consists of … Co|Fe|Co|Si … planes, i.e. every second plane is a Co plane separated by alternating Fe and Si planes. Three such motifs are required to produce the unit cell along this direction. It is worth mentioning that the CFS structure can be regarded as two superimposed zinc-blende (GaAs type) lattices, Co–Si and Co–Fe, shifted by half of the [1 1 1] diagonal of the conventional cubic unit cell. This together with the epitaxy with respect to the Si substrate gives a shared Si(1 1 1) interface plane between the film and substrate. The film bonding with Si is through the shared Si(1 1 1) plane from the Co–Si zinc-blende sub-lattice which leads to the following atomic plane stacking sequence in the interface vicinity: …Co|Fe|Co|Si|Si|Si|Si…, as shown schematically in figure 1(a). This particular atomic structure of the sharp interface with a shared Si plane is illustrated in figure 1(h) by presenting the atomic structure of CFAS on Si(1 1 1). Atomic relaxation analysis, obtained by DFT geometry optimization, shows that the first two Co atomic planes (region *s*4 in figure 1(a)) at the interface retain their bulk-like geometries, in contrast to the first Fe plane that shows ~33% relaxation (towards the substrate) compared to its bulk-like position. This demonstrates the strong interaction between Fe and Si in the interface region, indicating the Si–Fe bonds' hybridisation. In order to reveal the electronic structure of the sharp interface model, especially the influence of the interface on the CFS half-metallicity at the interface vicinity, we calculate

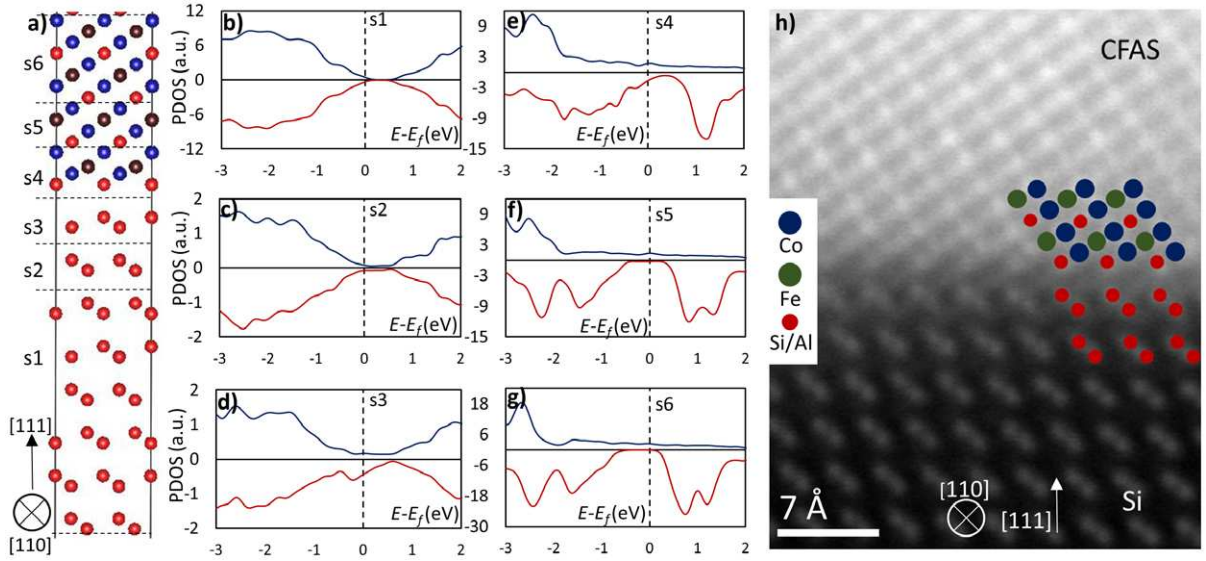

Figure 1. (a) Structural model of the abrupt CFS/Si interface shown along the [1 1 0] viewing direction. Red balls represent Si atoms, blue—Co, brown—Fe. (b)–(g) Spin polarized PDOS for the regions outlined in (a) and labelled as (*s*1)–(*s*6). Positive PDOS are for the spin-up states; negative for spin-down. (h) HAADF STEM image of the CFAS/Si interface imaged along the [1 1 0] direction, with overlaid structural model.

spin-polarized PDOS, figures 1(b)–(g). For clarity, we divide the interface into six regions, labelled as *s*1–*s*6 (figure 1(a)). The bulk 100% SP of the CFS electrode at the Fermi-level extends up to a fraction of the CFS unit cell at the interface (regions *s*5 and *s*6). However, the electronic structure is drastically different for regions *s*3 and *s*4, with SP values for these layers of −45% and +6% respectively. Therefore, the first third of the CFS unit cell (region *s*4) is almost non-polarized, while the first dumbbell layer of Si (region *s*3) has induced spin-polarization with the opposite sign to that of bulk CFS. These negative-spin states are very localized both in the interfacial Si (*s*3 region) and the CFS (*s*4 region) layers, figures 1(d) and (e). This deviation of SP at the interface can have a detrimental effect on the spin injection into the Si due to increased spin-scattering probability at the interface. A detailed insight of the contribution of different atomic species to the electronic structure discussed above can be obtained by comparing the PDOS of interface atoms to those in the bulk-like environment. Spin-polarized PDOS emerging from Co, Fe and Si atoms are shown in the supplementary figure S1 (stacks.iop.org/JPhysCM/28/395003/mmedia). The interface states arise due to the hybridisation between Si and Fe/Co atoms, which is also reflected in their relaxed geometric positions at the interface, as discussed above. The reversed spin-polarization at the interface also indicates that the magnetic moment of Fe and Co will be different compared to their values in the bulk. The calculations show that the magnetic moment of the interfacial Fe (region *s*4) is reduced (3.2 μ_B) compared to its bulk value of 3.3 μ_B. In addition, the Co magnetic moment decreases from 1.3 μ_B in the bulk to 1.0 μ_B over the first three Co atomic planes in the CFS. In order to investigate whether this effect is only limited to CFS electrodes, we perform the same sets of calculations for CFAS/Si and CMS/Si abrupt interfaces (see supplementary figures S2 and S3). For all cases, calculations show that reversed SP takes place at the interface.

From the above discussion it is clear that suitable interface atomic engineering is required in order to avoid the detrimental reversed SP. Achieving this goal would require thermodynamically stable monolayer(s) at the interface, that have similar structural lattice and elemental composition to the Heusler-electrode and Si. Chemically, when Co/Fe-based alloys are heterostructured with Si, formation of Co or Fe silicide can be energetically favourable. Although the atomic structure at the interface depends on the kinetic effects during the growth of the heterostructure, in order to estimate whether Co or Fe silicides are stable at the interface we calculated their formation energies. Among the number of Co and Fe silicides, $CoSi_2$ and Fe_3Si are of particular interest due to their crystal lattice match to that of CFS. For example, starting from the CFS structure, removing one Co sublattice and replacing the Fe sublattice by Si, leads to the $CoSi_2$ silicide; similarly, by replacing the two Co sublattices in CFS with Fe, the Fe_3Si silicide is obtained. First, we show that formation of Fe and Co silicides is more favourable than a sharp interface between CFS and Si. The difference in formation energies between (3CFS + 10Si) and (Fe_3Si + 6$CoSi_2$) is 5.1 eV in favour of the silicide's formation. Separate calculations show that the formation energy of $CoSi_2$ is −0.37 eV/atom, while for Fe_3Si is −0.35 eV/atom, which means that amongst the silicide phases which share similar lattice structure with that of the film and substrate, $CoSi_2$ is the most likely phase to be formed. Besides these general energetic considerations that point to the likely formation of a $CoSi_2$ phase, the relative atomic composition between the film and substrate also favours the $CoSi_2$ formation. In other words, the Co composition would gradually increase from zero in Si, one sub-lattice in $CoSi_2$, to two sub-lattices in CFS, in contrast to the Fe_3Si stoichiometry which would require a very high and abrupt gradient of the Fe concentration within several atomic planes at the interface. These conclusions for the stability of the $CoSi_2$ phase as an intermediate/interface

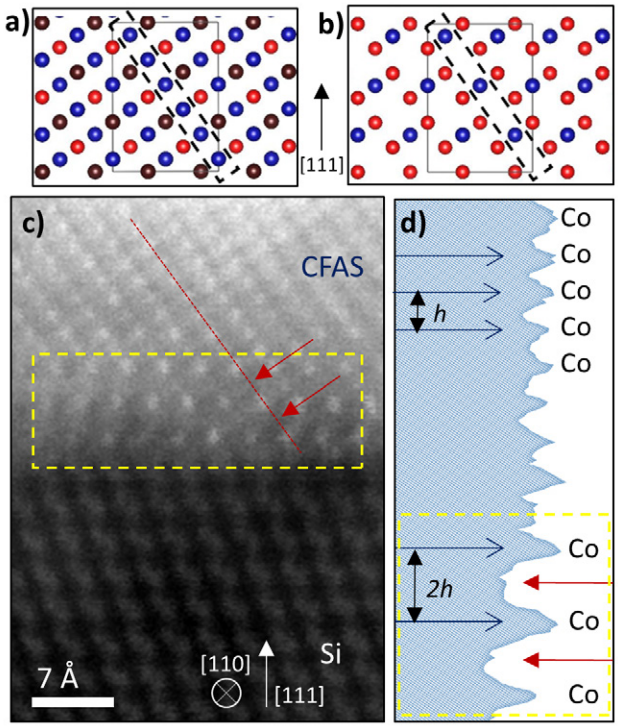

Figure 2. Structural models for bulk (a) CFS and (b) $CoSi_2$ (viewed along the [1 1 0] direction) showing the distinctive atomic plane stacking sequence along the [1 1 1] crystallographic direction. Dashed rectangles correspond to the red dotted line in (c) and outline that every second Co(1 1 1) plane from the CFS is not present in the $CoSi_2$ structure. Colour coding follows from figure 1. (c) HAADF STEM image of the CFAS/Si interface showing the presence of the $CoSi_2$ nano-island, outlined by the yellow dashed rectangle. (d) Intensity profile along the red line in (c) demonstrating the absence (in the region outlined by the yellow rectangle) of the Co atomic columns from the CFS structure, as expected for $CoSi_2$ structure. Blue arrows outline the Co atomic column positions, while red the positions of the missing Co atomic columns. This profile shows the 'h' and '2h' periodicity of Co atomic columns in the Heusler film and $CoSi_2$, respectively.

phase were further confirmed by the experimental verification of the formation of $CoSi_2$ nano-islands with thickness of 1–2 monolayers at the CFAS/Si interface, as shown in figure 2 (see also supplementary figure S4).

A natural next step is to investigate the effect of $CoSi_2$ (non-magnetic in the bulk form) layers on the interface SP. Interface stability of such layers on Si has been experimentally verified already by the growth of thick $CoSi_2$ films on Si [28]. Along the [1 1 1] direction, the $CoSi_2$ unit cell contains three Si–Co–Si monolayers (figure 2(b)). The atomic stacking of this characteristic Si–Co–Si monolayer is similar to Co–Fe–Co–Si layers in CFS with Fe planes replaced by Si and every second Co plane vacated (figures 2(a) and (b). Consideration of $CoSi_2$ interfacial layers with thicknesses larger than a unit cell would certainly not be of much benefit since bulk $CoSi_2$ has no spin-polarization and any interface proximity effects to CFS will be limited only to the interfacial layers.

First we consider an interface model with a single Si–Co–Si monolayer between Si and CFS, (figure 3(a)). Figures 3(b)–(g) shows the PDOS in the interface region from which the SP can be extracted. The inclusion of a Si–Co–Si monolayer has a profound effect on the SP across the interface, with the most striking feature being the recovery of the positive SP in all interface layers: in contrast to the abrupt interface, the first interface layers of the CFS (region *n*5) show only a slight reduction of SP while the Si–Co–Si monolayer has an induced positive spin-polarization (~45%). We note that the two interface bilayers of Si (*n*3 and *n*2 regions) also have a small positive spin density of states, which makes them positively SP at the Fermi level (~75%). In contrast to the abrupt CFS/Si, the insertion of Si–Co–Si monolayer fully recovers the positive SP of CFS in the interface region. This continuous high SP in the vicinity of the interface can significantly improve the injection of spin-polarized current, since the spin-scattering at the interface which was demonstrated for the sharp interface case is eliminated. The beneficial effect of Si–Co–Si on the electronic structure of the interface region is also reflected in the recovery of the bulk magnetic moment. In comparison to the sharp interface, which requires four atomic planes of Co in CFS to recover the bulk magnetic moment of 1.3 μ_B, the magnetic moment on Co atoms when the Si–Co–Si layer is introduced immediately reaches the bulk value except for the Co atoms in the first interface plane (1.0 μ_B). This in turn demonstrates the significant impact of the Si–Co–Si layer, which in essence provides an electronically and magnetically sharper interface in comparison to the structurally sharp CFS/Si interface. In addition to a single monolayer of Si–Co–Si, we also performed calculations for a double monolayer (supplementary figure S5) and a whole unit cell of $CoSi_2$ (3 monolayers). The beneficial effects of the Si–Co–Si monolayers decrease as the number of monolayers is increased. These results are not unexpected since a thick layer recovers the bulk properties of $CoSi_2$, a material that is non-magnetic and has no spin-polarization. Hence the practical implementation would require tailored growth of naturally occurring $CoSi_2$ with continuous single monolayer coverage on Si. We would like to note that the beneficial effect of the Si–Co–Si monolayer has also been confirmed for CFAS and CMS electrodes (supplementary figures S6 and S7).

Besides the SP in the interface vicinity, an additional important factor for spin injection is the position of the Fermi-level with respect to the semiconductor conduction band edge. The spin transport from the conduction band of CFS to the conduction band of Si will be more efficient if the difference between these two characteristic energies is smaller. The potential difference for the majority (resp. minority) electrons between the film and substrate is 2.8 eV (resp. 2.3 eV) for the abrupt CFS/Si interface, while for CFS/Si–Co–Si/Si they are 2.3 eV (resp. 1.8 eV). Therefore the presence of a Si–Co–Si monolayer lowers the average potential difference between the film and substrate by 0.5 eV (supplementary figure S8). By using the calculated potential difference we plot the band alignment (figure 4) for the two interface models. Figures 4(a) and (b) demonstrate that for the sharp interface model the Fermi-level is positioned just next to the valence band for Si (<0.1 eV energy difference). However, the energy shift of the bands by 0.5 eV upon the inclusion of a Si–Co–Si monolayer pins the Fermi-level in the substrate band gap far away from

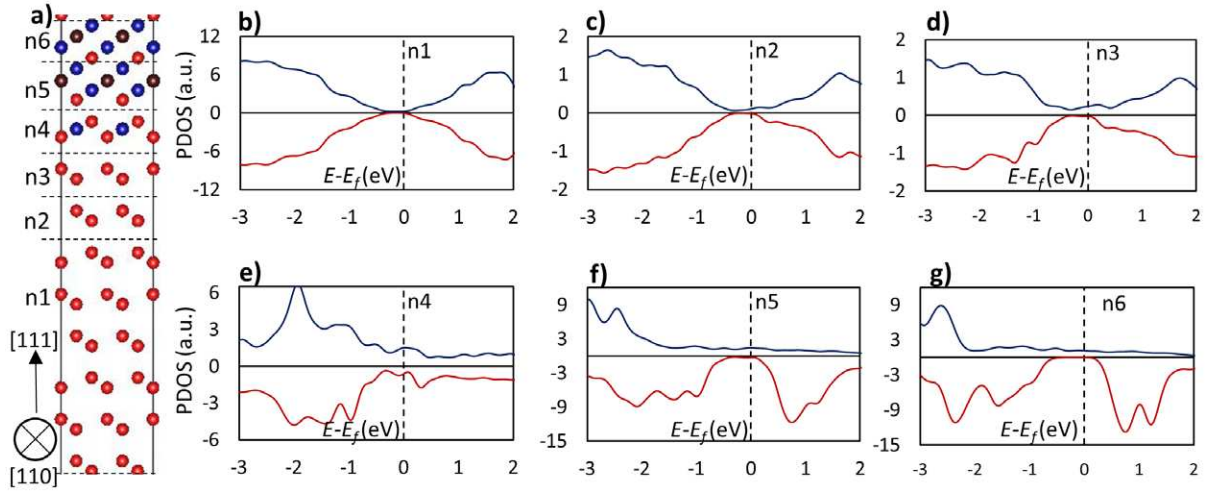

Figure 3. (a) Structural model of the CFS/Si–Co–Si/Si interface shown along the [1 1 0] viewing direction. Region *n*4 represents the Si–Co–Si monolayer. Red balls represent Si atoms, blue—Co, brown—Fe. (b)–(g) Spin polarized PDOS for the regions outlined in (a) and labelled as (*n*1)–(*n*6). Positive PDOS are for the spin-up states; negative for spin-down.

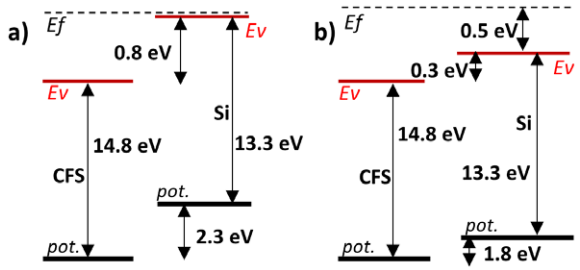

Figure 4. Band alignment drawing for the (a) abrupt CFS/Si and (b) CFS/Si–Co–Si/Si interface. Solid black and solid red lines stand for the average potentials and valence band edges for the minority spins, respectively. The Fermi-level is outlined by the dashed black line. Note that in (a) the energy difference between E_f and E_v is less than 0.1 eV.

the valence band edge. This decreases the energy difference which must be overcome in order to transfer the carriers from the film to the substrate, which in turn improves the spin injection properties.

In summary, first-principles calculations have shown that the spin-polarization is reversed at atomically sharp Co_2(Fe,Mn)(Al,Si)/Si(1 1 1) interfaces. Addition of a Si–Co–Si monolayer, the formation of which is shown to be thermodynamically favourable at the interface, recovers the positive spin-polarization of the Heusler/Si interface and creates an electronically and magnetically abrupt interface, the ultimate goal for spin injection into Si. In addition, this monolayer shifts the Fermi-level from the valence band edge (abrupt interface case) towards the conduction band edge of Si. The significantly improved half-metallicity and smaller energy difference (i.e. Schottky barrier height) between the conduction band edges of the Si and the Heusler film, make this interface highly desirable for device applications. Finally, this work shows that the Heusler/Si(1 1 1) interface's electronic properties are critically dependent on the atomic structure, which allows tailoring of their properties as demonstrated by the insertion of a Si–Co–Si monolayer at the interface.

Acknowledgments

This work has been supported by Engineering and Physical Sciences Research Council (EPSRC), through grants EP/K03278X/1 and EP/K032852/1. The authors are grateful for computational support from the UK national high performance computing service, ARCHER, for which access was obtained via the UKCP consortium and funded by EPSRC grant EP/K013564/1. The SuperSTEM Laboratory is the U.K. National Facility for Aberration-Corrected STEM, supported by the EPSRC.

Data availability

All data created during this research are available by request from the University of York Data Catalogue https://dx.doi.org/10.15124/89576114-1cf5-42f6-9536-5e94c80559dc.

References

[1] Jansen R 2012 *Nat. Mater.* **11** 400
[2] Žutić I, Fabian J and Das Sarma S 2004 *Rev. Mod. Phys.* **76** 323
[3] Felser C, Fecher G H and Balke B 2007 *Angew. Chem. Int. Ed.* **46** 668
[4] Katsnelson M I, Irkhin V Y, Chioncel L, Lichtenstein A I and de Groot R A 2008 *Rev. Mod. Phys.* **80** 315
[5] Schmidt G, Ferrand D, Molenkamp L W, Filip A T and van Wees B J 2000 *Phys. Rev.* B **62** R4790
[6] Furubayashi T, Kodama K, Sukegawa H, Takahashi Y K, Inomata K and Hono K 2008 *Appl. Phys. Lett.* **93** 122507
[7] Hirohata A, Sagar J, Lari L, Fleet L and Lazarov V 2013 *Appl. Phys.* A **111** 423
[8] Ishikawa T, Marukame T, Kijima H, Matsuda K-I, Uemura T, Arita M and Yamamoto M 2006 *Appl. Phys. Lett.* **89** 192505
[9] Lari L *et al* 2014 *J. Phys. D: Appl. Phys.* **47** 322003
[10] Sakuraba Y, Hattori M, Oogane M, Ando Y, Kato H, Sakuma A, Miyazaki T and Kubota H 2006 *Appl. Phys. Lett.* **88** 192508

[11] Taku I, Yuya S, Subrojati B, Kesami S, Seiji M and Koki T 2009 *Appl. Phys. Express* **2** 063003
[12] Tsunegi S, Sakuraba Y, Oogane M, Takanashi K and Ando Y 2008 *Appl. Phys. Lett.* **93** 112506
[13] Hamaya K, Hashimoto N, Oki S, Yamada S, Miyao M and Kimura T 2012 *Phys. Rev.* B **85** 100404
[14] Kimura T, Hashimoto N, Yamada S, Miyao M and Hamaya K 2012 *NPG Asia Mater.* **4** e9
[15] Dowben P A and Skomski R 2004 *J. Appl. Phys.* **95** 7453
[16] Yamada S, Tanikawa K, Oki S, Kawano M, Miyao M and Hamaya K 2014 *Appl. Phys. Lett.* **105** 071601
[17] Silvia P and Arthur J F 2007 *J. Phys.: Condens. Matter* **19** 315215
[18] Khosravizadeh S, Hashemifar S J and Akbarzadeh H 2009 *Phys. Rev.* B **79** 235203
[19] Nedelkoski Z, Hasnip P J, Sanchez A M, Kuerbanjiang B, Higgins E, Oogane M, Hirohata A, Bell G R and Lazarov V K 2015 *Appl. Phys. Lett.* **107** 212404
[20] Clark S J, Segall M D, Pickard C J, Hasnip P J, Probert M I J, Refson K and Payne M C 2005 *Z. Kristallogr.* **220** 567
[21] Chadov S, Fecher G H, Felser C, Minár J, Braun J and Ebert H 2009 *J. Phys. D: Appl. Phys.* **42** 084002
[22] Hasnip P J, Smith J H and Lazarov V K 2013 *J. Appl. Phys.* **113** 17B106
[23] Morris A J, Nicholls R J, Pickard C J and Yates J R 2014 *Comput. Phys. Commun.* **185** 1477
[24] Al-Allak H M and Clark S J 2001 *Phys. Rev.* B **63** 033311
[25] Oki S, Yamada S, Murakami T, Miyao M and Hamaya K 2012 *Thin Solid Films* **520** 3419
[26] Lari L, Lea S, Feeser C, Wessels B W and Lazarov V K 2012 *J. Appl. Phys.* **111** 07C311
[27] Gilks D *et al* 2016 *Sci. Rep.* **6** 20943
[28] Falke M, Falke U, Bleloch A, Teichert S, Beddies G and Hinneberg H-J 2005 *Appl. Phys. Lett.* **86** 203103